

**Supporting Information**

**Clickable Antifouling Polymer Brushes**

**for Polymer Pen Lithography**

*Uwe Bog,<sup>‡,∇</sup> Andres de los Santos Pereira,<sup>§,∇</sup> Summer L. Mueller,<sup>‡</sup> Shana Havenridge,<sup>‡</sup> Viviana Parrillo,<sup>§</sup> Michael Bruns,<sup>¶</sup> Andrea E. Holmes,<sup>‡</sup> Cesar Rodriguez-Emmenegger,<sup>\*,||</sup> Harald Fuchs,<sup>‡</sup> and Michael Hirtz,<sup>\*,†</sup>*

<sup>†</sup> Institute of Nanotechnology (INT) & Karlsruhe Nano Micro Facility (KNMF), Karlsruhe Institute of Technology (KIT), Germany

<sup>§</sup> Department of Chemistry and Physics of Surfaces and Biointerfaces, Institute of Macromolecular Chemistry ASCR, v.v.i., Czech Republic

<sup>‡</sup> Department of Chemistry, Doane University, Crete, Nebraska, and the Center for Nanohybrid Functional Materials (CNFM), University of Nebraska-Lincoln, USA

<sup>¶</sup> Institute for Applied Materials (IAM) & Karlsruhe Nano Micro Facility (KNMF), Karlsruhe Institute of Technology (KIT), Germany

<sup>||</sup> DWI – Leibniz Institute for Interactive Materials and Institute of Technical and Macromolecular Chemistry, RWTH Aachen University, Aachen, Germany

<sup>‡</sup> Physical Institute & Center for Nanotechnology (CeNTech), University of Münster, Germany

<sup>∇</sup> These authors contributed equally to this work.

## ADDITIONAL SURFACE PHYSICOCHEMICAL CHARACTERIZATION

### Additional XPS Spectra of the Initiator-Functionalized Surfaces

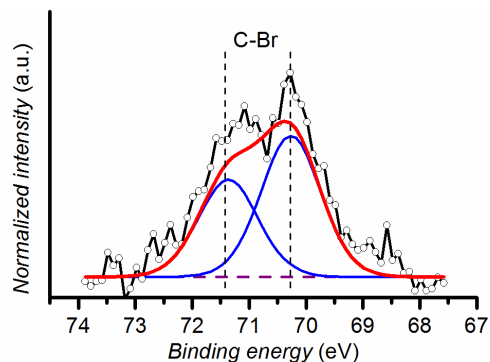


**Figure S1.** High-resolution XPS spectrum of the Br 3d binding energy region of the silane initiator ad-layer.

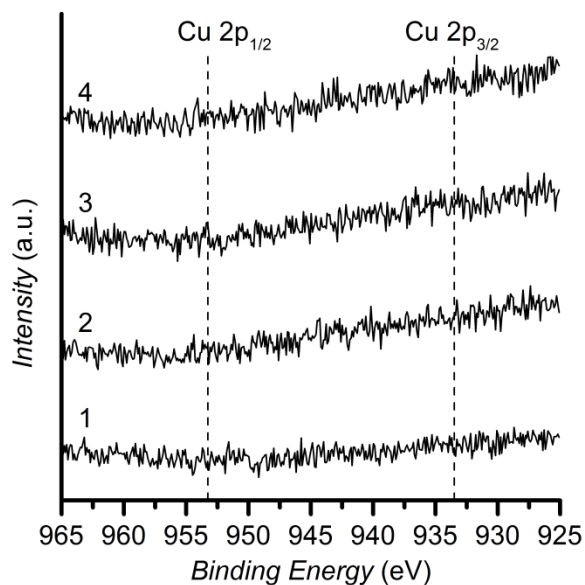


**Figure S2.** High-resolution XPS spectra of the Cu 2p binding energy region of ATRP initiator-SAM (1), poly(MeOEGMA) (2), poly(MeOEGMA-*b*-GMA) (3), and azide-functionalized poly(MeOEGMA-*b*-GMA) (4). The absence of signals demonstrates that the quantity of copper is below the detection limit of XPS.

## Characterization of the Azide-Functional Diblock Polymer Brushes via Fourier-Transform Infrared Spectroscopy (FTIR)

The success in the preparation of the targeted “clickable” antifouling diblock polymer brushes was further confirmed by chemical characterization of the layer using Infrared Reflection–Absorption Spectroscopy (IRRAS) FTIR. The spectrum was acquired on a brushes grafted from an  $\omega$ -mercaptoundecyl bromoisobutyrate initiator SAM on a gold-coated surface with a Nicolet Nexus 870 spectrometer equipped with a SAGA reflection attachment (Thermo Fisher Scientific, Czech Republic), using 256 scans at a resolution of  $4\text{ cm}^{-1}$ .

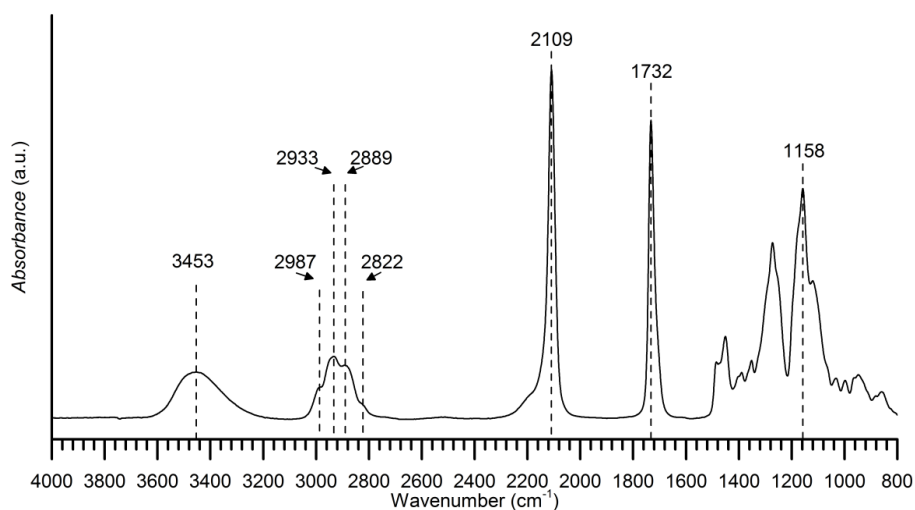


**Figure S3.** Infrared reflection-absorption spectrum of an azide-functionalized poly(MeOEGMA-*b*-GMA) (thicknesses of 20 and 16 nm for the poly(MeOEGMA) and poly(GMA) blocks, respectively).

The spectrum obtained for an azide-substituted poly(MeOEGMA-*b*-GMA), where the thicknesses of the poly(MeOEGMA) and poly(GMA) block are 20 and 16 nm, respectively, is shown in Figure S3. Importantly, IRRAS-FTIR measurements. The strongest band is visible at  $2109\text{ cm}^{-1}$  and is assigned to the antisymmetric stretching mode of the azide groups present in the top block of the polymer brush. The second strongest contribution to the spectrum appears at  $1732\text{ cm}^{-1}$  and has its origin in the C=O stretching mode of the ester groups, present all along the polymer chains and coming from the methacrylate groups. The main contribution in the fingerprint region is found at  $1158\text{ cm}^{-1}$  and originates from the C–O–C stretching mode of the oligo(ethylene glycol) side chains of the poly(MeOEGMA). The C–H region is characterized by the presence of four bands at:  $2987\text{ cm}^{-1}$  (CH<sub>3</sub> asymmetric stretching),  $2933$  and  $2889\text{ cm}^{-1}$  (CH<sub>2</sub> asymmetric and symmetric stretching, respectively), and at  $2822\text{ cm}^{-1}$  (O–CH<sub>3</sub> stretching, characteristic for the terminal groups of the oligo(ethylene glycol) side chains of the poly(MeOEGMA) block). The broad band at  $3453\text{ cm}^{-1}$  arises from the OH groups, abundant in the poly(GMA) block after ring opening upon substitution with azide.

## Additional Adherence Characterization

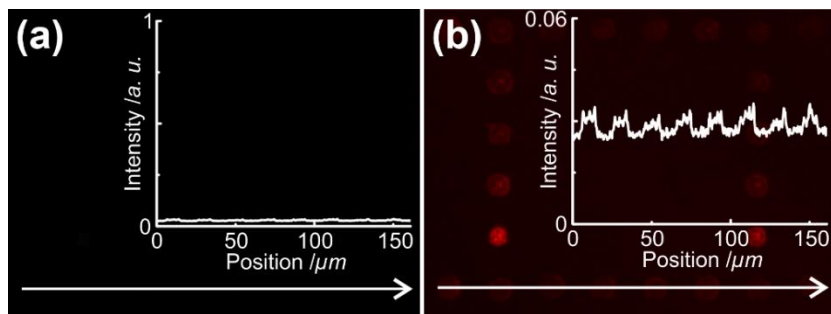


**Figure S4.** Negative control for click-chemistry binding on glass. (a) After rinsing almost all TAMRA-DBCO is removed from the non-functionalized glass sample (exposure time 2s). (b) Shows the image in (a) with adjusted contrast settings. Insets represent intensity profiles along eight features.

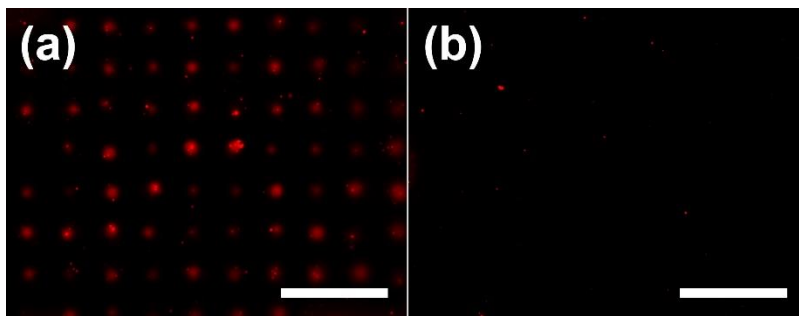


**Figure S5.** Negative control for click-chemistry binding on brushes. (a) Print of TAMRA-azide on an azide-functionalized brush and (b) same sample after rinsing (exposure time 6s). Scale bars equal 100  $\mu\text{m}$ .

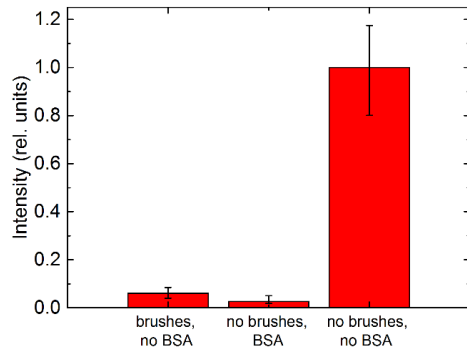


**Figure S6.** Relative background fluorescence of samples after streptavidin-cy3 incubation. Samples covered with brushes or blocked with BSA (“brushes, no BSA” and “no brushes, BSA”, respectively) prior to incubation show low background in comparison to a bare glass (“no brushes, no BSA”).

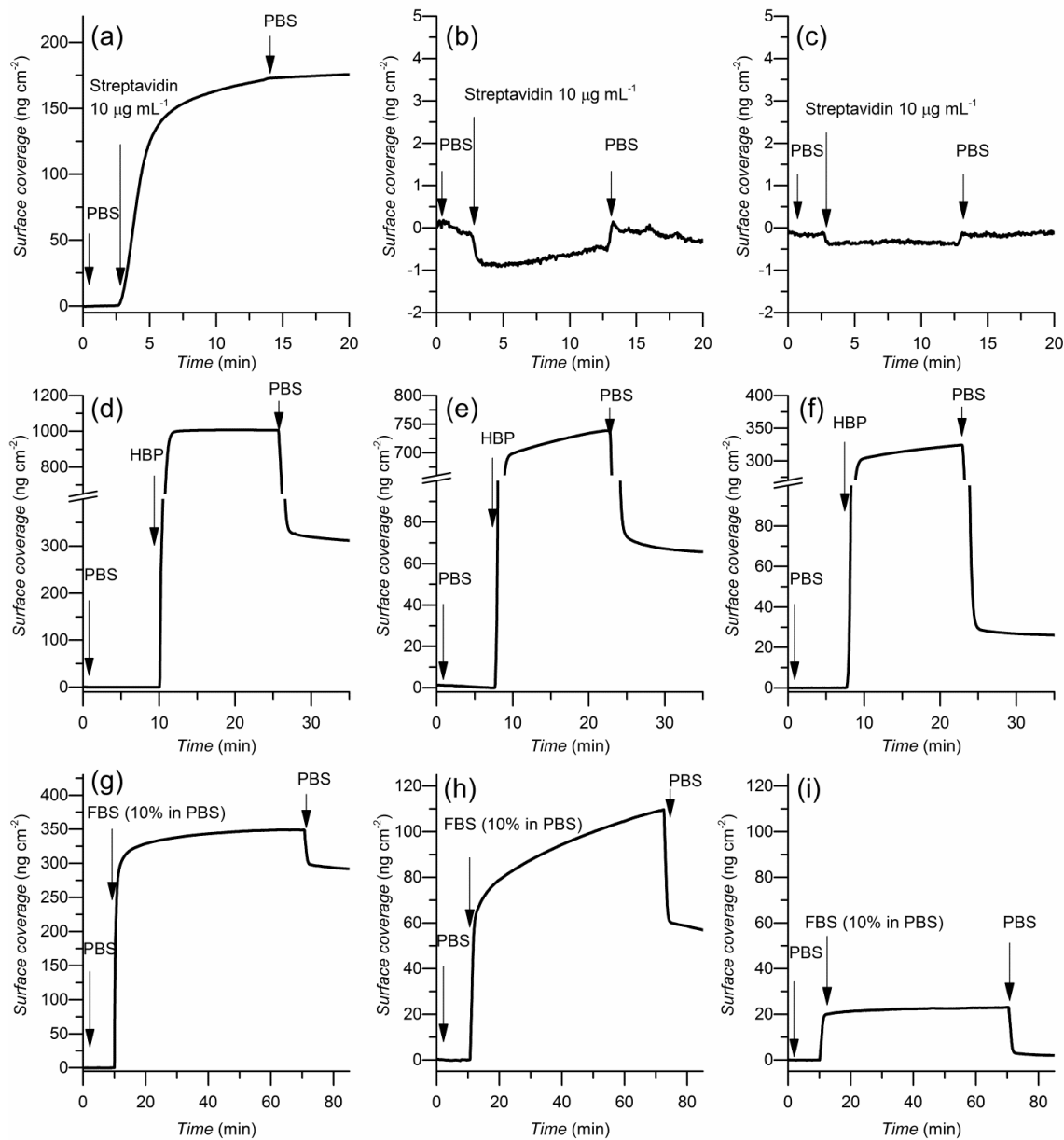


**Figure S7.** Non-specific adsorption (fouling) measured by surface plasmon resonance on bare gold from  $10 \mu\text{g mL}^{-1}$  streptavidin in PBS (a), undiluted human blood plasma (d), and 10% fetal bovine serum in PBS (g); on BSA-passivated surfaces from  $10 \mu\text{g mL}^{-1}$  streptavidin in PBS (b), undiluted human blood plasma (e); and 10% fetal bovine serum in PBS (h); and on diblock polymer brush-coated surfaces from  $10 \mu\text{g mL}^{-1}$  streptavidin in PBS (c), undiluted human blood plasma (f); and 10% fetal bovine serum in PBS (i). Note: the non-specific protein adsorption value is read from the graphs as the difference in SPR resonant wavelength in buffer before and after contact with the analyzed protein solution. The immediate shifts in resonant wavelength seen upon injection of the solution are caused by the change in bulk refractive indices and are not indicative of adsorption.